Heliyon 10 (2024) e39773

Contents lists available at ScienceDirect

Heliyon

journal homepage: www.cell.com/heliyon

Research article

Coir fibre-reinforced concrete for enhanced compressive strength and sustainability in construction applications

Krishna Prasad Guruswamy **, Senthilkumar Thambiannan, Arputharaj Anthonysamy, Kirti Jalgaonkar, Ajinath Shridhar Dukare, Ravi Pandiselvam *, Naveenkumar Jha

ICAR- Central Institute for Research on Cotton Technology (CIRCOT), Mumbai, 400019, India

ARTICLE INFO

Keywords:
Coir fibre
Fibre volume fraction
Fibre length
Response surface methodology
Reinforced concrete

ABSTRACT

This research explores the potential of coir fibre as a sustainable and effective reinforcement material to enhance the compressive strength (CS) of concrete. The influence of the fibre volume fraction (FVF) and fibre length (FL) on the CS of the coir fibre reinforced concrete was studied using the response surface method (RSM). The selected range for the FVF was from 4 % to 12 %, and the FL varied from 0.4 cm to 1.2 cm, as per the experimental design. The research determined that the coir fibre with an FVF of 4 % and an FL of 10 mm yielded the maximum CS for the reinforced concrete cubes, measuring 34 N/mm^2. Furthermore, an increase in fibre content was observed to lead to a decrease in the workability of coir fibre-reinforced concrete. Furthermore, Fourier transform infrared spectroscopy (FTIR) and X-ray diffraction (XRD) analyses of the control and coir fibres extracted from the concrete cubes after a period of 1 year indicated no significant changes in the functional properties, thermal properties and crystallinity of the fibres.

1. Introduction

The construction industry is a well-recognized contributor to various environmental challenges, including air pollution, climate change, drinking water contamination, and substantial landfill waste [1]. Recent research by Bimhow revealed that this sector is responsible for 23 % of air pollution, 50 % of climate change impacts, 40 % of drinking water pollution, and 50 % of landfill waste [2]. Additionally, the U.S. the Green Building Council predicted a notable increase of 1.8 % in emissions from commercial buildings by 2030 [3]. The severity of these environmental threats has prompted growing interest in exploring sustainable solutions to mitigate the environmental footprint of the construction industry, including the utilization of natural fibres.

As the primary building material in construction, concrete plays a pivotal role in shaping the environmental impact of the industry [4,5]. However, traditional concrete often lacks the desired mechanical properties required for sustainable and environmentally friendly construction. To address this limitation, researchers have sought to enhance concrete performance by incorporating natural fibres [6]. In recent years, steel fibres have been a popular choice for reinforcing concrete structures [7–10], and numerous studies have consistently demonstrated that the introduction of fibres significantly improves the compressive strength (CS) of concrete [11,12]. However, the extensive use of steel fibres has raised concerns because of their nonrenewable nature, depletion of availability,

* Corresponding author.
** Corresponding author.
E-mail addresses: gurukris1@gmail.com (K.P. Guruswamy), r.pandiselvam@icar.gov.in, anbupandi1989@yahoo.co.in (R. Pandiselvam).

https://doi.org/10.1016/j.heliyon.2024.e39773
Received 29 June 2024; Received in revised form 22 October 2024; Accepted 23 October 2024
Available online 24 October 2024
2405-8440/

energy-intensive production processes, and associated costs. Consequently, natural fibers have emerged as promising and sustainable alternatives, offering the benefits of renewability, lower energy requirements, and cost-effectiveness.

Numerous natural fibres, including jute [13], hemp [14], banana [15], coir [16], flax [17,18], sisal [19,20], bamboo [21], sugarcane bagasse [22], and kenaf [23], have been investigated to enhance the mechanical properties of concrete [5]. However, previous studies have reported varying results. For instance, Syed et al. [24] reported that the addition of processed coir fibre to concrete decreased workability but increased CS by 0.6 % or decreased it by 1.2 %. Maia et al. [25] found that the CS of rendering mortar decreased with an increased content and length of coir fibres. Li et al. [26] revealed that chemically treated coir fibre-reinforced mortar exhibited superior strength and reduced weight compared to conventional mortar. Similarly, Chin et al. [27] reported that the decrease in slump values with increase in Basalt fibre content. Poongodi et al. [28] explored the impact of coir fibres and recycled aggregate on the bond strength of pavement quality concrete, concluding that up to 1 % coir fibres could be added without compromising CS. Sharma and Sheikh [29] focused on self-compacting reinforced concrete and determined that the incorporation of 2 % coir fibres improved the CS. Hwang et al. [30] found that adding coir fibres, along with a high water-to-cement ratio, lowered the CS of cement composites. Senthilkumar et al. [31] explored the impact of fibrillation on coconut fibres in epoxy composites and observed enhanced tensile strength and damage resistance with fibrillated fibres. Ali et al. [32] discovered that incorporating 5 cm coconut fibres in concrete improved workability and mechanical properties.

India is a major producer of coir fibre, with a production of approximately 280,000 metric tons of coir fibre in the year 2021-22 [33], and has also witnessed its widespread application as a reinforcing material in concrete. While substantial research has been conducted on regression models for predicting textile-based material properties [34,35], there is a lack of studies specifically examining the effects of fibre length and volume fraction on the CS of coir fibre-reinforced concrete. This study employs the response surface method (RSM) to analyze the compressive properties of reinforced concrete cubes, considering different combinations of fibre length and volume fraction.

2. Research significance

The integration of coir fibres into concrete represents a relatively recent and promising development that deserves further exploration. This research holds particular significance because it focuses on systematically evaluating the outcomes of experiments conducted on coir fibre-reinforced concrete cubes. Specifically, it investigated the impact of two critical parameters, fibre length (ranging from 0.4 cm to 1.2 cm) and volume fraction (ranging from 4.00 % to 12.00 %), on the CS of these concrete specimens. By scrutinizing the influence of these variables, this study contributes to a deeper understanding of the potential improvements in concrete performance achievable through the addition of coir fibres.

The application of a quadratic model, derived from an optimal design within the framework of Response Surface Methodology (RSM), allows for the precise prediction of the 28-day CS of concrete. This approach not only offers valuable insights into the performance of concrete reinforced with coir fiber, but also provides a basis for optimizing the properties of the material. As the construction industry seeks sustainable and environmentally friendly solutions, the findings of this research may play a pivotal role in advancing the use of coir fibres as a viable and eco-conscious reinforcement material. Furthermore, this study helps expand the body of knowledge surrounding natural fibre-reinforced concrete, potentially opening doors for innovative and environmentally responsible construction practices.

3. Experimental program

3.1. Cement

In this study, VICAT OPC 53 grade cement was used, a widely used building material in India. The cement employed in this study had a specific gravity of 3.15 and a 28-day CS of no less than 53 N/mm^2. The cement composition included lime (61.85 %), silica (20.07 %), alumina (5.32 %), iron oxide (4.62 %), insoluble residues (<4.0 %), magnesia (0.83 %), sulfuric anhydride (2.50 %), chloride (0.0028 %) and alkali (0.1 %).

3.2. Aggregates

Coarse aggregates of 20 mm and 10 mm and fine aggregate (sand) were used. Table 1 presents their physical properties. Sieve analysis, following BIS IS 2386–1:1963 (R2016) is illustrated in Fig. 1.

Table 1
Physical properties of coarse and fine aggregates [IS 383 (2016)].

Specifications	Coarse aggregates		Fine aggregates
	10 mm	20 mm	
Specific gravity	2.8	2.82	2.59
Water Absorption (%)	1.82	1.59	3.85

3.3. Coir fibre

Untreated coir fibres with an average length of 155.8 mm were used in this study. Based on previous research [28–32], trials were initially conducted for 4 % FVF with coir fibres of lengths 1.25, 2.5, and 5.0 cm. From the results, it was observed that the 1.25 cm coir fibre length exhibited a better CS (29.8 N/mm^2) than the 2.5 cm (25.4 N/mm^2) and 5 cm (20.9 N/mm^2) coir fibre lengths. It was also observed that a larger coir length agglomerated during mixing with cement and coarse aggregates. However, no agglomeration was found in the 1.25 cm coir length. Based on the above observation, 1.2 cm was selected for further studies through an optimal (custom) design of the experiment by varying the length of the fiber and FVF in the concrete mix. A coir fibre length of 1.2 cm was prepared using a hammering machine. To obtain different coir fibre lengths, hammered coir fibres were fibrillated through a double disc refiner using gap settings of 7, 10, 13, 15, 20, and 25 thou were used. The raw coir fibre and the coir fibres produced in various gaps are shown in Fig. 2.

3.4. Experimental design and statistical analysis

The response surface methodology (RSM) was used to determine the optimal fibre length (FL) and fibre volume fraction (FVF) and to investigate their effects on the CS of coir fibre-reinforced concrete. The experiment was laid down with two independent factors at seven levels, using an optimal (custom) design. The independent variables were FL (0.40 cm, 0.52 cm, 0.58 cm, 0.69 cm, 0.86 cm, 0.92 cm, and 1.2 cm) and FVF (4 %, 5.2 %, 5.76 %, 6.88 %, 8.6 %, 9.2 %, and 12 %) (Table 2). The total number of experimental runs (Table 3) was 14 (five lack of fit points, three replicate points, and six model points). The effects of the independent variables on the CS were determined. A pragmatic model of the quadratic multiple regression equation (1) suggested by the software was used to predict the CS of concrete using an optimally customized design.

$$\mathrm{Y} = \beta_0 + \beta_1\beta X_1 + \beta_2\beta X_2 + \beta_3\beta X_1^2 + \beta_4\beta X_2^2 + \beta_5 X_1 X_2 \tag{1}$$

where Y is the response variable, with X1 and X2 as inputs, and βo to β5 as regression coefficients. Data analysis was done using Design Expert 9.0.7 (Stat-Ease Inc.). ANOVA evaluated fiber length and volume fraction with quadratic models. Model adequacy was checked by the lack-of-fit test and R^2, and non-significant terms were excluded for better prediction.

Based on the optimal (custom) design, a mix design for M25 grade concrete as IS 456 (2000), was obtained (Table 3). Subsequently, cement, coarse aggregates, fine aggregates, and coir fibres were mixed manually in the dry stage, and then water and admixture (Supercon 300) were added, maintaining a water-to-cement ratio of 0.53.

3.5. Experimental test

Based on the mix design, a concrete mix was prepared (Fig. 3.) and a slump test was conducted. Later a total of 9 concrete cubes (150 x 150 × 150 cm^3) for each sample were cast. The concrete cubes were then removed from the mold after 24 h. Furthermore, the de-molded cubes were placed in water. From each sample, three cubes were tested for CS at 7, 14, and 28 d of curing according to the Indian Standard [IS 456:2000 (Reaffirmed in 2021)]. For comparison, a control concrete cube without coir fibre was prepared and tested as per the standard. Scanning electron microscopy (SEM), Fourier transform infrared spectroscopy (FTIR), X-ray diffraction (XRD), and thermogravimetric analysis (TGA) of the optimized sample.

3.6. Surface morphology and functional groups analysis

The surface morphology of the cement-reinforced coir fibre was studied using SEM (Philips XL30, Philips, Netherlands). The coir

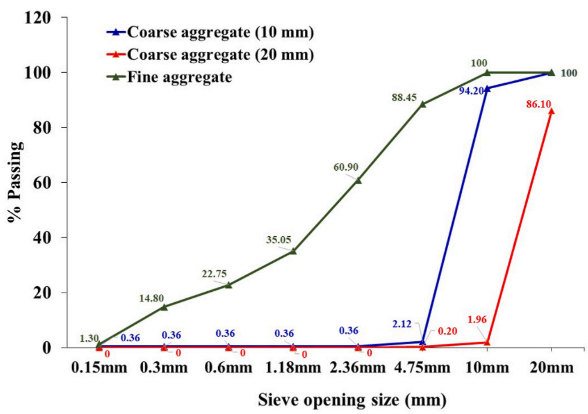

Fig. 1. Particle size distribution of coarse aggregates (10 mm, 20 mm) and fine aggregates.

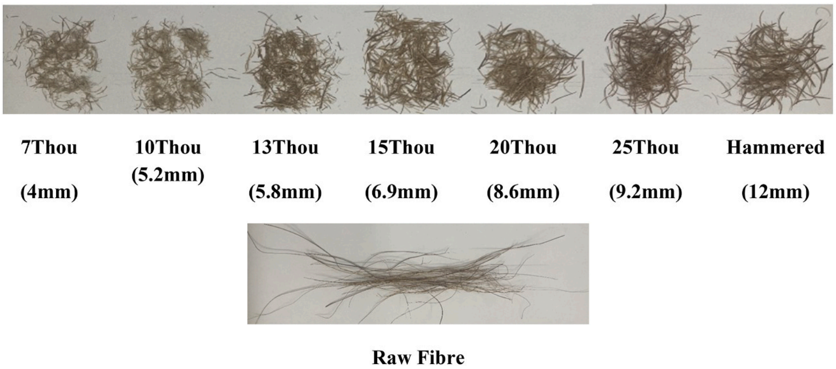

Fig. 2. Raw and fibrillated coir fiber in various settings of the double disc refiner.

Table 2
Level of variables considered for the preparation of coir fibre reinforced concrete by Optimal (Custom) Design.

Variable	Name	Variable Level	
		−1	1
A	Fibre length (FL) (cm)	0.4	1.2
B	Fiber volume fraction (FVF) (%)	4	12

Table 3
Ingredients of concrete mix.

Run Order	Fibre length (FL) (cm)	Fiber volume fraction (FVF) (%)	Fiber (kg/m^3)	Coarse aggregate (kg/m^3)		Fine aggregate (kg/m^3)	Cement (kg/m^3)	Amount of water used (L)
				10 mm	20 mm			
Control	0	0	0	552	588	896	320	172.8
1	0.86	8.60	24.76	504				
2	1.20	8.60	24.76	504				
3	1.20	12.00	34.55	486				
4	0.40	4.00	11.51	530				
5	0.58	9.20	26.49	501				
6	1.20	5.20	14.97	523				
7	0.40	6.88	19.81	514				
8	0.86	12.00	34.55	486				
9	0.86	8.60	24.76	504				
10	1.20	5.20	14.97	523				
11	0.92	5.76	16.58	520				
12	0.86	8.60	24.76	504				
13	0.52	12.00	34.55	486				
14	0.69	4.00	11.51	530				

fibre samples were subjected to attenuated total reflectance ATR-FTIR spectroscopy using a Shimadzu IR Prestige-21® spectrophotometer.

3.7. X-ray diffraction (XRD)

To understand the change in the crystallinity of the control and hammered coir fibres, XRD was carried out using an X-ray diffractometer (M/s Ultima IV, Rigaku, Japan). The cement-reinforced coir fibre was removed from the concrete after a one-year period of casting to study the change in the crystallinity of this extracted coir fibre compared with the control coir fibre sample.

3.8. Thermogravimetric analysis (TGA)

The thermal degradation behavior of the cement-reinforced coir fibre was analyzed using a Netzsch TG 209 F3 Tarsus® thermal analyzer and compared with a control coir fibre sample.

Fig. 3. Process followed for preparation of coir fibre reinforced concrete cubes.

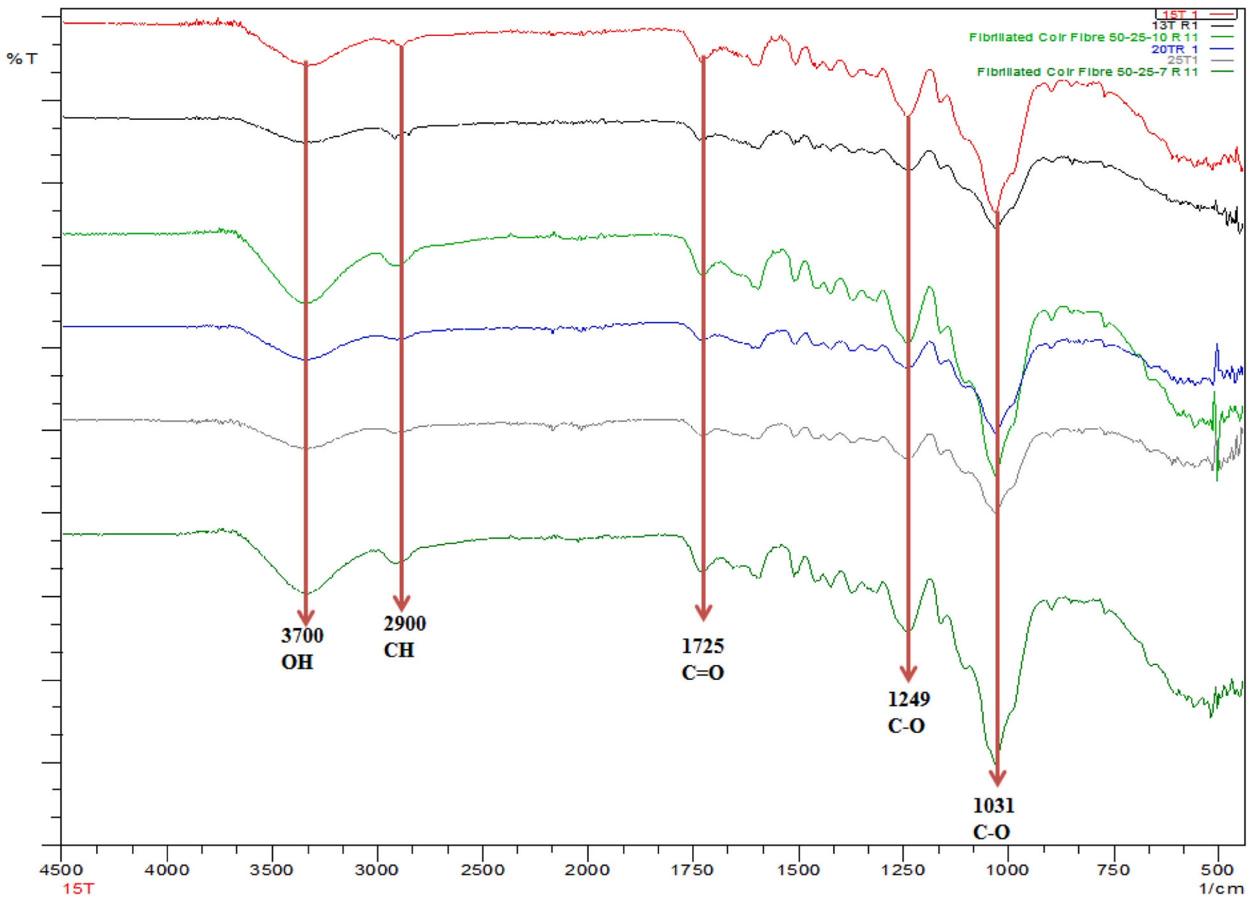

Fig. 4. FTIR spectra of hammered coir fibre and refined coir fibres at different spacing. XRD analysis of hammered fibre and refined coir fibre.

4. Results and discussions

4.1. FTIR analysis of hammered coir fibre and refined coir fibre

The IR transmittance bands of the control hammered fibre and coir samples refined under various conditions are depicted in Fig. 4. As anticipated, all fibres exhibited characteristic peaks corresponding to three natural polymers: cellulose, lignin, and xylan. The analysis revealed minimal variation in the IR spectrum between the hammered fibre and samples refined under different conditions. Notably, the transmittance band ranging from 3600 to 3700 cm^{-1} can be attributed to hydroxyl group stretching within the cellulose polymer of the coir fibre. Another distinct transmittance band at 2900 cm^{-1} corresponds to the CH group stretching in the cellulose molecular chain. The minor peak at 1725 cm^{-1} signifies the presence of carbonyl (C=O) and acetyl groups in hemicellulose. The 1249 cm^{-1} band corresponds to C-O stretching, indicating lignin in coir fibre. A distinct peak at 1509 cm^{-1} is associated with the aromatic skeletal vibration of C=O in lignin. The 1031 cm^{-1} band represents C-O stretching within the cellulose chain [36,37].

Coir is a natural fiber from the coconut industry. Cellulose I, derived from natural and microbial sources, consists of two crystalline forms: cellulose Iα and Iβ. In the XRD pattern, cellulose I shows characteristic diffraction peaks at 14.9°, 16.5°, 20.5°, 22.7°, and 34.5°, corresponding to reflection planes 110, 110, 012, 002, and 004 [38].

Fig. 5 shows the XRD diffraction pattern of the coir fibres (control) and the different types of fine powders created by maintaining a spacing of 7thou, 13thou, 15thou, 20thou, and 25thou between the two discs. The main crystalline peak at 22.3°–22.5° 2θ corresponded to cellulose (002). Lower-intensity peaks observed between 15.4°-16.3° and 34.7°–35° 2θ, attributed to cellulose (101) and (004), respectively, suggested a higher presence of amorphous materials like lignin and hemicellulose in the coir [39]. No notable changes in the XRD pattern were observed after mechanical grinding of the fine powders, confirming that there was no significant alteration in crystal size or morphology. The XRD analysis further validated the presence of cellulose Iα and cellulose Iβ [40].

4.2. Effect of coir fibre on workability of concrete mix

From Table 4, it was evident that the FVF exerts a compelling influence on the workability of the concrete mix. Specifically, as the FVF content increased from 5.2 % to 12 % at a fibre length of 1.2 cm, the workability decreased from 75 mm to 55 mm. This indicates that even for the same fibre length, the workability of the concrete mix was significantly affected by the fibre volume fraction.

To a certain extent, the fibre length also affects the workability of the concrete mix. No significant difference in workability was observed for 8.6 % of the FVF at fibre lengths of 1.2 cm and 0.86 cm. However, significant differences were noted for fibre lengths of 1.2 cm and 0.52 cm for the same FVF. It was found that reducing the fibre length to half of its original length influences the workability of the concrete mix, even for the same FVF. This could be due to the hydrophilic nature of the coir fibre, which might absorb water and result in reduced workability [41]. Additionally, the high air content in the concrete mix might also contribute to reduced workability in the case of a high fibre length and high volume fraction [42].

4.3. Compressive strength (CS) of coir fibre reinforced concrete cubes

An Optimal custom design for two independent variables, Fibre Length (0.4 cm–1.2 cm) and FVF (4%–12 %) with seven levels each, was utilized to create the model. The CS of each combination are tabulated in Table 5. A quadratic model was employed to determine the individual and interaction effects of independent variables on the dependent variable (CS). The model for CS was found to be highly significant ($p \leq 0.01$) with a high coefficient of determination ($R^2 \geq 0.75$). (Table 6). The ANOVA results in Table 6 indicate that there was no interaction effect between the independent and dependent variables. However, only the individual effects were observed. The ANOVA results indicated that the FVF and fibre length significantly influenced the CS of the concrete cube, as evidenced by the highly significant p-values (<0.05). The second-order quadratic model was found to be the best fit for the experimental data, and the

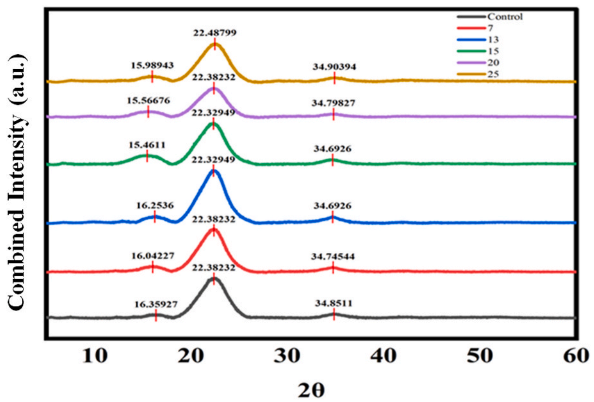

Fig. 5. XRD graphs of Coir fibre (control) and its different type of fine powders.

Table 4
Workability of samples based on run order.

Run Order	Fibre length (FL) (cm)	Fiber volume fraction (FVF) (%)	Slump
Control	0.00	0.00	90
1	0.86	8.60	60
2	1.20	8.60	60
3	1.20	12.00	55
4	0.40	4.00	84
5	0.58	9.20	62
6	1.20	5.20	75
7	0.40	6.88	65
8	0.86	12.00	55
9	0.86	8.60	61
10	1.20	5.20	72
11	0.92	5.76	72
12	0.86	8.60	62
13	0.52	12.00	60
14	0.69	4.00	74

Table 5
Independent variables and results for the preparation of the coir fibre reinforced concrete.

Run Order	Fibre length (FL) (cm)	Fiber volume fraction (FVF) (%)	28-Day Compressive Strength (N/mm^2)	Predicted Compressive Strength (N/mm^2)	Residuals
Control	0.00	0.00	29.2	–	–
1	0.86	8.60	31.0	30.33	0.67
2	1.20	8.60	29.7	30.04	−0.34
3	1.20	12.00	29.3	28.54	0.76
4	0.40	4.00	28.0	27.54	0.46
5	0.58	9.20	30.0	27.84	2.16
6	1.20	5.20	32.0	31.54	0.46
7	0.40	6.88	25.0	26.27	−1.27
8	0.86	12.00	27.3	28.83	−1.53
9	0.86	8.60	30.4	30.33	0.07
10	1.20	5.20	31.0	31.54	−0.54
11	0.92	5.76	31.5	31.76	−0.26
12	0.86	8.60	30.2	30.33	−0.13
13	0.52	12.00	25.6	25.85	−0.25
14	0.69	4.00	31.0	31.27	−0.27

Table 6
ANOVA for the quadratic model for Compressive Strength.

Source	p-value	Remark
Model	0.0057	Significant
Fiber Length	0.0012	
Fiber Volume Fraction	0.0054	
Fiber Length* Fiber Volume Fraction	0.7649	Not significant
Fiber length [2]	0.0161	
Fiber Volume Fraction [2]	0.6108	Not significant
Standard Deviation	1.03	
Mean	29.43	
CV%	3.51	
R [2]	0.8256	
Adjusted R^2	0.7731	
Predicted R^2	0.6690	
Adequate Precision	10.6994	

regression equation was developed as follows:

$$\text{Compressive strength} = 20.25 - 0.44{*}\text{FVF} + 28.27{*}\text{Fibre Length} - 14.13{*}\textit{Fibre Length}^2 \quad (2)$$

As shown in Fig. 6 (a), the interaction effect between the FVF and its length on the CS of the concrete cubes was insignificant. As shown in Fig. 6 (b), the CS of the concrete cubes continuously decreased as the FVF increased from 4 % to 12 %. Furthermore, as the FVF increased from 4 % to 6.9 % for a fibre length of 0.40 cm, a 10.71 % reduction in CS was observed. Similarly, a reduction in CS of 7–12 % was observed when the FVF increased from 8.6 % to 12 % for fibre lengths of 0.86 cm and 1.2 cm. The reduction in the CS can

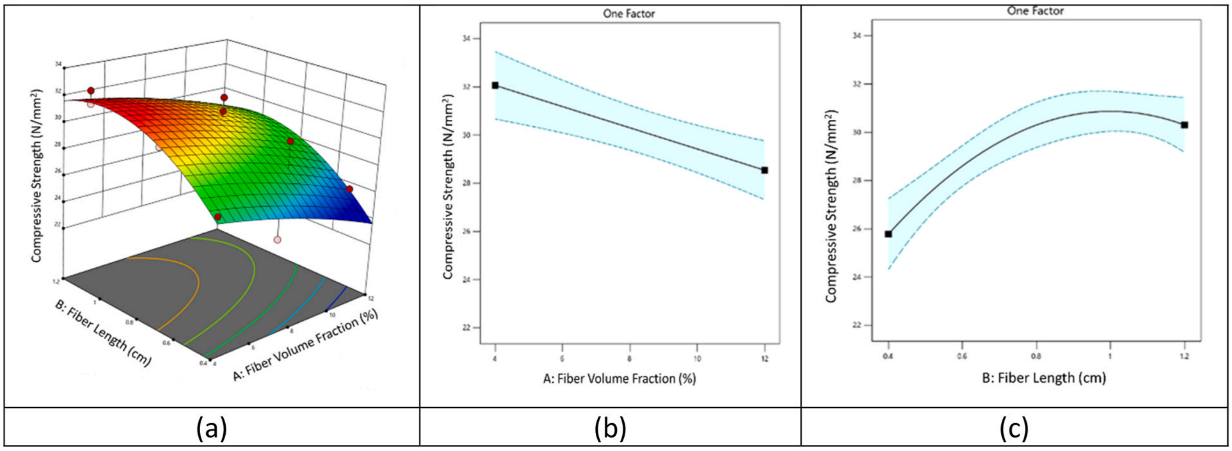

Fig. 6. Graphical representation of (a) 3-D response surface interactive effects of varied A (FVF) and B (fibre length); (b) Impact of A (FVF) on 28-day CS; (c) Impact of B (fibre length) on 28-day CS.

be attributed mainly to the reduction in the workability of the concrete owing to the hydrophilic nature of the coir fibre, which absorbs water. As the fibre absorbs water, it reduces the water content during the preparation of concrete, affecting the interfacial bonding of cement with other ingredients during the curing process. This, in turn, negatively affects the CS of the coir fibre-reinforced concrete.

Along with fibre volume fraction, fibre length significantly affects the CS of concrete. Fig. 6(c) illustrates that as the length of the reinforced coir fibres increased, the CS of the concrete cube also improved. Notably, the CS increased when the fibre length ranged from 0.4 to 1.2 cm. However, at a fibre length of 1.0 cm, the CS saturated and decreased above that value as the FVF increased. It should be noted that fibres with a shorter length (less than 0.5 cm) do not meet the CS standard of IS 456. It serves only as a filler and does not resist the load, which negatively affects the CS of the cube. All other coir fibre lengths >0.58 cm meets the CS standard of IS 456.

4.4. Optimization of fibre length and fibre volume fraction for preparation of coir fibre reinforced concrete cubes

The optimum conditions for the coir fibre-reinforced concrete cube were analyzed using Design Expert software. The optimum conditions for the coir fibre-reinforced concrete cube was obtained to be 1.0 cm of fibre length and fibre volume fraction of 4 %. At the optimum point, a concrete cube was prepared and the CS was determined. The predicted (33 N/mm^2) and experimental (34 N/mm^2) values showed no significant difference between them. The fibre extracted from the optimized concrete cube was also examined by SEM, and its morphological structure is shown in Fig. 7. This figure depicts the surface roughness of the coir fibre developed by fibrillation of the hammered coir fibre. The surface roughness helps in interlocking the fibre with concrete ingredients, resulting in strong interfacial bonding between the fibre and concrete mix. This improved bonding ultimately enhanced the CS of the coir fibre-reinforced concrete.

4.5. FTIR analysis of control hammered coir fibre and fibre extracted from concrete cube

A comparison between the FTIR spectra of the hammered coir fibre and coir fibres extracted from the concrete cube prepared under the optimized conditions is presented in Fig. 8. The analysis revealed that the coir fibre used in the creation of the concrete cube consisted of three distinct polymers: cellulose, hemicelluloses, and lignin. This observation suggested that the natural polymers did not undergo significant disintegration during the process. Notably, FTIR analysis identified two new distinct and well-defined peaks at 1400 cm^{-1} and 870 cm^{-1}. These peaks are attributed to the absorption caused by out-of-plane bending at approximately 870 cm^{-1} and the asymmetric stretch at approximately 1400 cm^{-1}, which correspond to the carbonate ions present in calcium carbonate [43]. The appearance of these peaks is likely a result of traces of calcium carbonate introduced into the material during the extraction of coir fibres from the cement cube [44].

The XRD diffraction patterns of the coir fibres (control) and extracted coir fibres of the concrete cube are shown in Fig. 9. The main crystalline peak 2θ at 22.4°–22.5° corresponds to cellulose (002). The lower-intensity peak observed 2θ at 15.5–16° and 34.7–34.9°, corresponding to cellulose (101) and (004), respectively, indicate a higher amount of amorphous material, such as lignin and hemicellulose, in the coir [39]. The cubic coir fibre XRD graph shows an extra peak 2θ at 29.07°, which is due to the presence of calcium carbonate in the cubic fibre [45]. The XRD graphs of the control and cubic coir fibres confirmed the presence of cellulose Iα and cellulose Iβ [40].

4.6. TGA analysis

Fig. 10 depicts the thermogravimetric analysis (TGA) of the coir fibres employed in the manufacture of concrete cubes, revealing

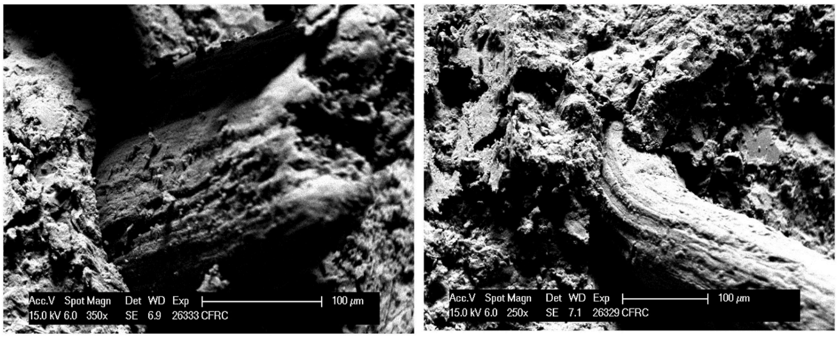

Fig. 7. SEM micrographs of cement reinforced coir fibres.

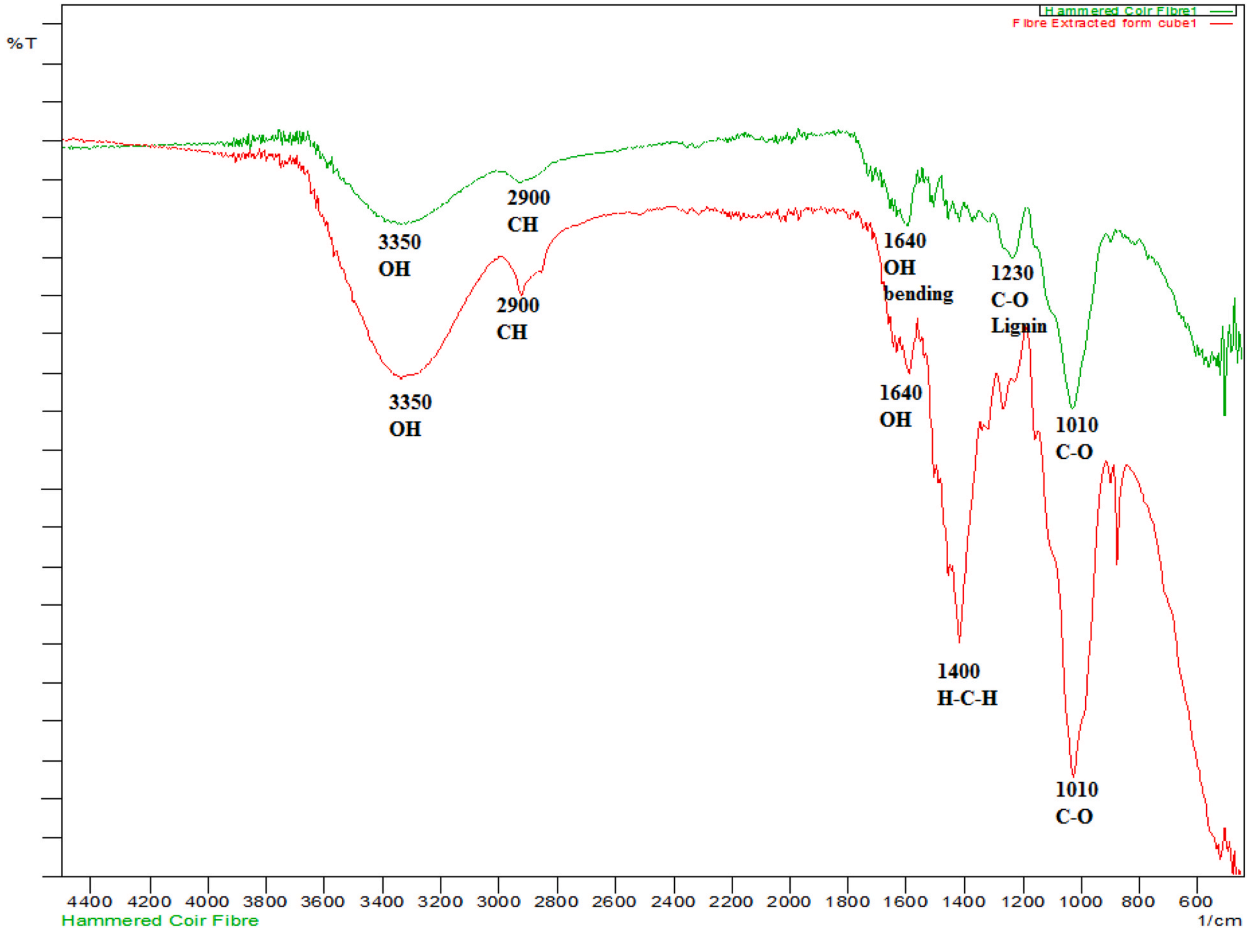

Fig. 8. FTIR spectra of hammered coir fibre and fibres extracted from the concrete cube. XRD analysis of control hammered coir fibre and fibre extracted from concrete cube.

distinctive degradation patterns observed in three distinct regions. Initially, a minor weight loss (2.5 %) was observed, which was primarily attributed to the evaporation of moisture content inherent in the coir fibre. Subsequently, cellulose degradation became evident within the temperature range of 300–380 °C, leading to significant weight loss in the coir fibre. Notably, the analysis indicated a comparable degradation pattern between the control fibres and those extracted from the concrete cube, suggesting that the stability of the coir fibres remained largely unchanged throughout the process. However, a notable observation emerged regarding the fibre extracted from the cube, which showed a higher residual mass. This phenomenon could be attributed to the adherence of calcium carbonate, as corroborated by the findings of the XRD and FTIR analyses. The presence of calcium carbonate significantly influenced the residual mass of the coir fibres extracted from the cement cubes.

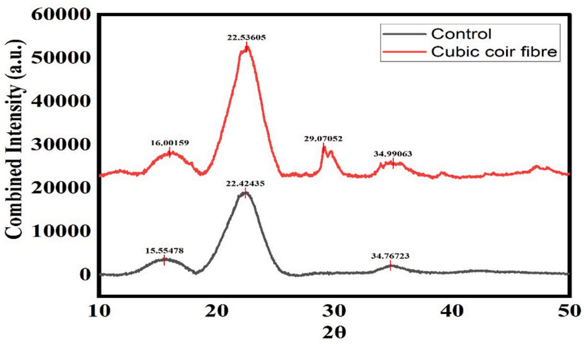

Fig. 9. XRD pattern of hammered coir fibre and fibres extracted from the concrete cube.

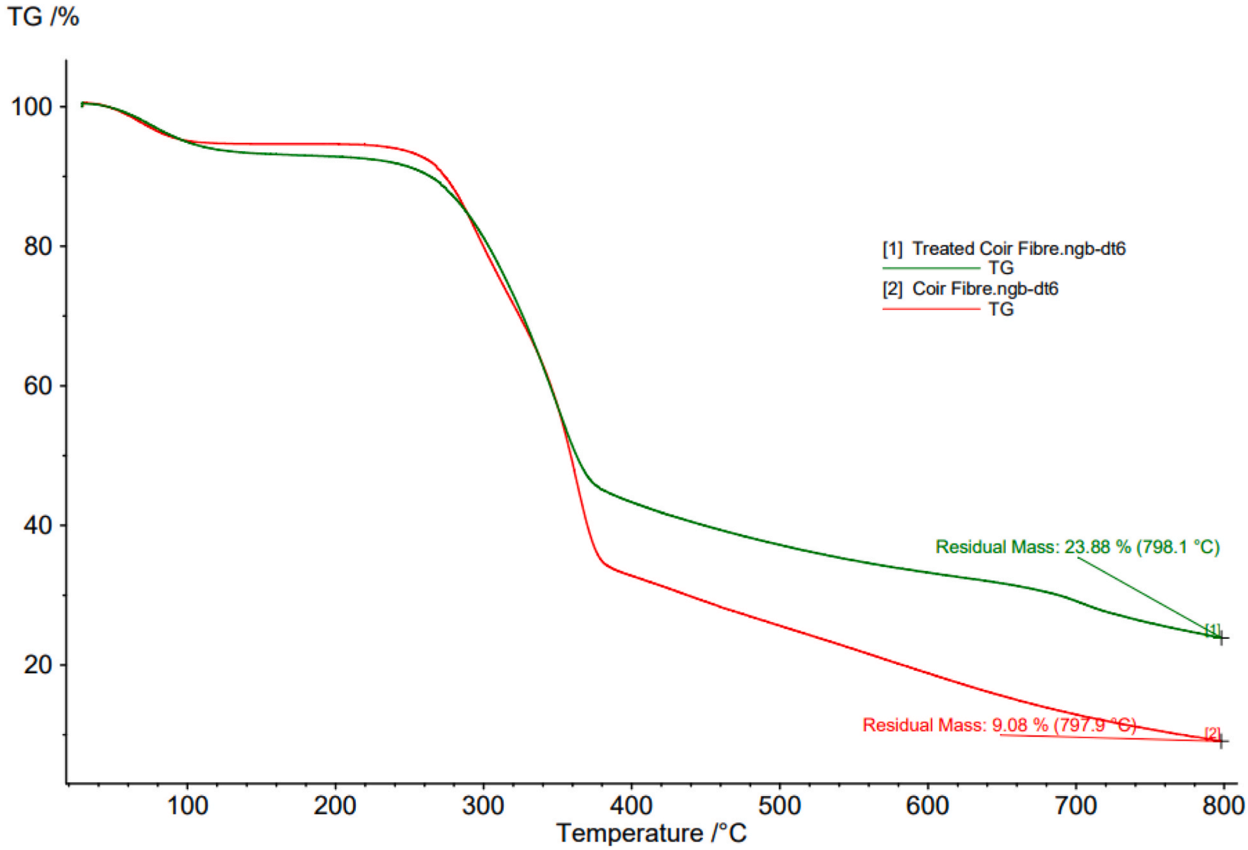

Fig. 10. TGA of hammered coir fibre and fibres extracted from the concrete cube.

5. Conclusions

The study revealed a notable impact of fibre length (FL) and fibre volume fraction (FVF) on the CS of coir fibre-reinforced concrete. The highest CS was achieved with a fibre length of 1.0 cm and a fibre volume fraction of 4.0 %. This optimized condition gives a 34 MPa CS of the coir fibre-reinforced concrete. The compression test of the concrete cubes indicated that the CS decreased as the FVF increased from 4 % to 12 % owing to the lower bonding between the cement and other ingredients because of the high water absorption by the coir fibre. In addition to the CS, the FVF highly influences the workability of the concrete mix owing to the hydrophilic nature of the coir fibre. However, FL affects workability to some extent. The FTIR, XRD, and TGA analyses showed that the stability of the coir fibre in concrete remained largely unchanged for a period of one year compared with raw coir fibre. This study provides valuable insights into the optimal conditions for enhancing the CS of coir fibre-reinforced concrete, offering a sustainable and effective solution for the construction industry. By carefully balancing the trade-offs between CS, workability, and the key parameters of FVF and FL, this study contributes to the growing body of knowledge regarding natural fibre-reinforced concrete, paving the way for more environmentally conscious and efficient construction practices.

CRediT authorship contribution statement

Krishna Prasad Guruswamy: Writing – review & editing, Writing – original draft, Resources, Conceptualization. **Senthilkumar Thambiannan:** Methodology, Investigation. **Arputharaj Anthonysamy:** Methodology, Investigation. **Kirti Jalgaonkar:** Methodology, Investigation. **Ajinath Shridhar Dukare:** Methodology, Investigation. **Ravi Pandiselvam:** Writing – original draft, Software, Resources, Methodology, Investigation, Funding acquisition. **Naveenkumar Jha:** Writing – original draft, Methodology, Investigation, Formal analysis, Data curation.

Declaration of competing interest

The authors declare the following financial interests/personal relationships which may be considered as potential competing interests:The corresponding author is an Advisory Board Member of Heliyon-Ravi Pandiselvam. If there are other authors, they declare that they have no known competing financial interests or personal relationships that could have appeared to influence the work reported in this paper.

Acknowledgements

Indian Council of Agricultural Research (ICAR), New Delhi, India is duly acknowledged for providing funds under CRP on Natural Fibre Project.

References

[1] Miller A. The surprising effects of construction on the environment.The surprising effects of construction on the environment. Published June 13, 2020. https://www.theenvironmentalblog.org/2020/06/surprising-effects-of-construction-environment/.
[2] K. Dobrowolska, How does construction affect the environment? ARCHDESK, Published June 13, https://archdesk.com/blog/how-does-construction-affect-the-environment/, 2021.
[3] S. Sikra, How does construction impact the environment?, Published June 13, https://gocontractor.com/blog/how-does-construction-impact-the-environment/, 2024. (Accessed 13 June 2024).
[4] J.M. Crow, The concrete conundrum, The concrete conundrum (2024). Published June 13, https://www.chemistryworld.com/features/the-concrete-conundrum/3004823. (Accessed 13 June 2024).
[5] A. Geremew, P. De Winne, T.A. Demissie, H. De Backer, Treatment of Natural Fiber for Application in Concrete Pavement, vol. 2021, 2021, https://doi.org/10.1155/2021/6667965.
[6] Ahamed MS, Ravichandran P, Krishnaraja AR. Natural fibers in concrete – A Review. 1055:1-8.doi:10.1088/1757-899X/1055/1/012038.
[7] M. Gholhaki, G. Pachideh, O. Rezayfar, An experimental study on mechanical properties of concrete containing steel and polypropylene fibers at high temperatures, Journal of Structural and Construction Engineering 4 (3) (2017 Nov 22) 167–179.
[8] G. Pachideh, M. Gholhaki, An experimental investigation into effect of temperature rise on mechanical and visual characteristics of concrete containing recycled metal spring, Struct. Concr. 22 (1) (2021 Feb) 550–565.
[9] G. Pachideh, M. Gholhaki, A. Moshtagh, Performance of concrete containing recycled springs in post-fire conditions, Proceedings of the Institution of Civil Engineers-Structures and Buildings 173 (1) (2020 Jan) 3–16.
[10] G. Pachideh, M. Gholhaki, Using steel and polypropylene fibres to improve the performance of concrete sleepers, Proceedings of the Institution of Civil Engineers-Structures and Buildings 173 (9) (2020 Sep) 690–702.
[11] E. Poveda, G. Ruiz, H. Cifuentes, R.C. Yu, X. Zhang, Influence of the fiber content on the compressive low-cycle fatigue behavior of self-compacting SFRC 101 (2017), https://doi.org/10.1016/J.IJFATIGUE.2017.04.005.
[12] S. Blasón, E. Poveda, G. Ruiz, H. Cifuentes, A. Fernández Canteli, Twofold Normalization of the Cyclic Creep Curve of Plain and Steel-Fiber Reinforced Concrete and its Application to Predict Fatigue Failure, vol. 120, 2019, https://doi.org/10.1016/J.IJFATIGUE.2018.11.021. G. Fraunhofer, Less moisture in natural fibres, Science News (2018), https://www.sciencedaily.com/releases/2018/02/180202123924.htm/. (Accessed 2 February 2018).
[13] S.P. Kundu, S. Chakraborty, S. Chakraborty, S. Chakraborty, Effectiveness of the surface modified jute fibre as fibre reinforcement in controlling the physical and mechanical properties of concrete paver blocks 191 (2018), https://doi.org/10.1016/J.CONBUILDMAT.2018.10.045.
[14] E.A. E Awwad, B. Hamad, M. Mabsout, H. Khatib, Sustainable concrete using hemp fibres, Proceedings of the Institution of Civil Engineers-Construction Materials 166 (1) (2013 Feb) 45–53, https://doi.org/10.1680/coma.11.00006.
[15] A. Afraz, M. Ali, Effect of banana fiber on flexural properties of fiber reinforced concrete for sustainable construction, Engineering Proceedings 12 (1) (2021 Dec 30) 63, https://doi.org/10.3390/engproc2021012063.
[16] V.S. Uday, B. Ajitha, Concrete reinforced with coconut fibres, International Journal of Engineering Science and Computing 7 (4) (2017) 10436.
[17] C. Yaremko, Durability of Flax Fibre Reinforced Concrete (Doctoral Dissertation, University of Saskatchewan), 2012.
[18] G.B. Abdallah, Strengthening of structures by composite materials based on jute and flax fibers, Academic Journal of Civil Engineering 40 (1) (2022 Jun 8) 211–214.
[19] M.P. Iniya, K. Nirmalkumar, A review on fiber reinforced concrete using sisal fiber, in: InIOP Conference Series: Materials Science and Engineering, vol. 1055, IOP Publishing, 2021 Feb 1 012027, 1.
[20] F. de A. Silva, B. Mobasher, R.D.T. Filho, Cracking mechanisms in durable sisal fiber reinforced cement composites, Cement Concr. Compos. 31 (10) (2009), https://doi.org/10.1016/J.CEMCONCOMP.2009.07.004.
[21] S.M. Dewi, M.N. Wijaya, N.C. Remayanti, in: The Use of Bamboo Fiber in Reinforced Concrete Beam to Reduce Crack, vol. 1887, AIP Publishing LLC AIP Publishing, 2017, https://doi.org/10.1063/1.5003486.
[22] F.S. Khalid, H.S. Herman, N.B. Azmi, Properties of sugarcane fiber on the strength of the normal and lightweight concrete, in: InMATEC Web of Conferences, vol. 103, EDP Sciences, 2017 01021.
[23] A. Guo, Z. Sun, J. Satyavolu, Experimental and finite element analysis on flexural behavior of mortar beams with chemically modified kenaf fibers, Construct. Build. Mater. 292 (2021 Jul 19) 123449.
[24] H. Syed, R. Nerella, S.R. Madduru, Role of coconut coir fiber in concrete, Mater. Today: Proc. 27 (2020 Jan 1) 1104–1110.
[25] C. Maia Pederneiras, R. Veiga, J. de Brito, Physical and mechanical performance of coir fiber-reinforced rendering mortars, Materials 14 (4) (2021 Feb 9) 823, https://doi.org/10.3390/ma14040823.

[26] Z. Li, L. Wang, X. Wang, Flexural characteristics of coir fiber reinforced cementitious composites, Fibers Polym. 7 (2006 Sep) 286–294.
[27] S.C. Chin, I.G. Shaaban, J.P. Rizzuto, S.U. Khan, D. Mohamed, N.I.M. Roslan, A. Abdul Aziz, Predictive models for mechanical properties of hybrid fibres reinforced concrete containing bamboo and Basalt fibres, Structures 61 (2024) 106093, https://doi.org/10.1016/j.istruc.2024.106093.
[28] K. Poongodi, P. Murthi, P. Revathi, Influence of coir fibre and recycled aggregate on bond strength of pavement quality concrete, Mater. Today: Proc. 61 (2022 Jan 1) 400–405.
[29] U. Sharma, I.M. Sheikh, Investigating self-compacting-concrete reinforced with steel & coir fiber, Mater. Today: Proc. 45 (2021 Jan 1) 4948–4953.
[30] C.L. Hwang, V.A. Tran, J.W. Hong, Y.C. Hsieh, Effects of short coconut fiber on the mechanical properties, plastic cracking behavior, and impact resistance of cementitious composites, Construct. Build. Mater. 127 (2016 Nov 30) 984–992.
[31] T. Senthilkumar, A.K. Bharimalla, C. Sundaramoorthy, P.G. Patil, N. Vigneshwaran, Fibrillation of coconut fibers by mechanical refining to enhance its reinforcing potential in epoxy composites, Fibers Polym. 21 (2020 Sep) 2111–2117.
[32] M. Ali, A. Liu, H. Sou, N. Chouw, Mechanical and dynamic properties of coconut fibre reinforced concrete, Construct. Build. Mater. 30 (2012 1) 814–825, https://doi.org/10.1016/j.conbuildmat.2011.12.068.
[33] M. Jawaid (Ed.), Coir Fiber and its Composites: Processing, Properties and Applications, Elsevier, 2022.
[34] S. Debnath, M. Madhusoothanan, V.R. Srinivasamoorthy, Prediction of air permeability of needle-punched nonwoven fabrics using artificial neural network and empirical models, Indian J. Fiber Textil Res. 255 (2000) 251–255.
[35] D.C. Montgomery, G.C. Runger, N.F. Hubele, Engineering Statistics, John Wiley & Sons, 2009 Jul 27.
[36] B.S. Yew, M. Muhamad, S.B. Mohamed, F.H. Wee, Effect of alkaline treatment on structural characterisation, thermal degradation and water absorption ability of coir fibre polymer composites, Sains Malays. 48 (3) (2019) 653–659, https://doi.org/10.17576/jsm-2019-4803-19.
[37] P.S. Sari, P. Spatenka, Z. Jenikova, Y. Grohens, S. Thomas, New type of thermoplastic bio composite: nature of the interface on the ultimate properties and water absorption, RSC Adv. 5 (118) (2015) 97536–97546, https://doi.org/10.1039/C5RA16311K.
[38] N. Lin, A. Dufresne, Surface chemistry, morphological analysis and properties of cellulose nanocrystals with gradiented sulfation degrees, Nanoscale 6 (10) (2014) 5384–5393.
[39] O. Ayeni, A.A. Mahamat, N.L. Bih, T.T. Stanislas, I. Isah, H. Savastano Junior, E. Boakye, A.P. Onwualu, Effect of coir fiber reinforcement on properties of metakaolin-based geopolymer composite, Appl. Sci. 12 (11) (2022) 5478.
[40] A.D. French, Idealized powder diffraction patterns for cellulose polymorphs, Cellulose 21 (2) (2014) 885–896.
[41] O. Onuaguluchi, N. Banthia, Plant-based natural fibre reinforced cement composites: a review, Cement Concr. Compos. 68 (2016) 96–108.
[42] M.Z. Bayasi, P. Soroushian, Effect of steel fiber reinforcement on fresh mix properties of concrete, Materials Journal 89 (4) (1992 Jul 1) 369–374, https://doi.org/10.14359/9751.
[43] N.A. Sommerdijk, G.D. With, Biomimetic CaCO3 mineralization using designer molecules and interfaces, Chem. Rev. 108 (11) (2008 Nov 12) 4499–4550.
[44] E.V. Tararushkin, T.N. Shchelokova, V.D. Kudryavtseva, A study of strength fluctuations of Portland cement by FTIR spectroscopy, in: InIOP Conference Series: Materials Science and Engineering 2020 Sep 1, vol. 919, IOP Publishing. and engineering, 2020 022017, https://doi.org/10.1088/1757-899X/919/2/022017, 919.
[45] E. E Dalas, P.G. Klepetsanis, P.G. Koutsoukos, Calcium carbonate deposition on cellulose, J. Colloid Interface Sci. 224 (1) (2000 Apr 1) 56–62, https://doi.org/10.1006/jcis.1999.6670.